Using existing infrastructure to transform urban district heating systems to renewable energy supply

Ulrich Trabert, Isabelle Best, Weena Bergstraesser, Oleg Kusyy, Janybek Orozaliev, Klaus Vajen

University of Kassel, Institute of Thermal Engineering, Kassel (Germany)

Abstract

In this case study the integration of a river water heat pump at an existing combined heat and power plant was examined with the aim to achieve a 50 % renewable cover ratio in the district heating system of an urban district. Three different concepts were designed in line with the requirements of the German subsidy program "Wärmenetzsysteme 4.0". Furthermore, the integration of decentralized solar thermal rooftop systems was analyzed regarding the suitable rooftops in the district and the potential feed-in into the district heating system. A focus of the conducted dynamic 15-year simulation with the software energyPRO is on electricity market price induced heat production. The relevant components include the operation of the heat pump and a storage, but also additional combined heat and power and power-to-heat units. The heat supply concepts are compared in terms of operational characteristics and economic efficiency.

Keywords: Urban district heating, transformation process, river water heat pump, decentralized solar thermal systems, levelized cost of heat

Abbreviations:

CHP	Combined heat and power	LCoH	Levelized cost of heat
COP	Coefficient of performance	PtH	Power-to-heat
DH	District heating	SPF	Seasonal performance factor
FLH	Full load hours	TTES	Tank thermal energy storage

1. Introduction

Urban district heating (DH) systems in Germany today are usually large 2nd or 3rd generation networks with more than 100 km route length and supply temperatures in the range of 90 °C up to 120 °C (Frederiksen and Werner, 2017; Schweikardt et al., 2012). An important first step to transform those networks to 4th generation DH systems is the reduction of network temperatures to promote the efficient integration of renewable energies. To initiate this transformation process, it can be beneficial to implement subnetworks in the most suitable areas of a large heating network for a smooth transition to smart thermal energy systems. According to AGFW e.V. (2019), 80 % of the heat distributed via heating networks in 2018 was produced in combined heat and power (CHP) processes. With coal and gas fired power plants phasing out of operation in the next decades, new use cases need to be developed for the existing infrastructure. Those sites bear the potential to advance the interaction between the heat and electricity sector. The shift from a sole production site to a more flexible operation as a prosumer supports the integration of renewable energies into the electricity grid by reducing the required electrical storage capacity. At the same time, the exploitation of environmental heat by heat pumps requires electricity. A common feature of centralized CHP plants located close to cities are river water cooling systems. The associated infrastructure and permissions for river water usage enable an easy integration of environmental heat into urban DH systems. In this paper a techno-economic analyses of three different concepts for this use case is conducted with a focus on electricity market price induced heat production.

2. Case study

This case study is about a district in the center of a German city with an existing DH network. The framework for the investigation is given by the German subsidy program "Wärmenetzsysteme 4.0" (heating network systems 4.0) according to BAFA (2020). The program is aimed at promoting the development of new smart thermal energy

doi:10.18086/eurosun.2020.02.05 Available at http://proceedings.ises.org

networks, but also at transforming existing DH networks. The key requirement of the program is that at least 50 % of the heat supply is to be covered by renewable energies.

2.1 Boundary conditions of the urban district

The district is a densely populated area with mostly multi-family houses, but also some commerce and industry. More than 70 % of the building stock connected to the DH network has been built before the year 1960 and more than 40 % even before 1918. The mean specific heat demand of the residential buildings is around 100 kWh/(m²·a), including space heating and domestic hot water. In total, the residential heat demand amounts to 29.2 GWh/a, while the non-residential heat demand is about 8.6 GWh/a. It is expected that the heat demand of the current customers will decrease due to renovation measures and rising mean ambient temperatures. Nevertheless, the district bears sufficient potential for new heating network connections. It is assumed that the reduction in heat demand is continually compensated through customer acquisition in the future. In addition, a nearby new housing development with around 12.8 GWh/a heat demand is supposed to be connected to the DH network until 2030. This leads to the heat demand scenario depicted in Fig. 1.

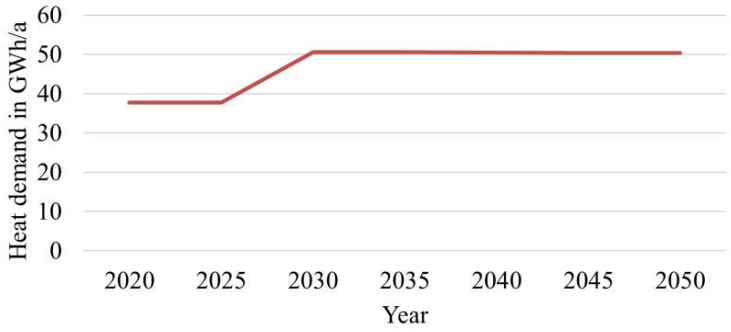

Fig. 1 Heat demand development from 2020 to 2050

There is one main supply line of the heating network leading into the district, which is the only connection of the district to the main heat supplier, the CHP power plant. This juncture can be used to create a subnetwork with lower operating temperatures compared to the high temperature primary network. At the same time, the CHP power plant is located next to a river. The route length of the subnetwork is around 15.2 km, so that the linear heat demand density is 2.5 MWh/(m_{route}·a) today. Due to the mentioned extensions of the grid in the heat demand scenario, the linear heat density decreases to 2.2 MWh/(m_{route}·a) until the year 2038.

2.2 Integration of a river water heat pump

The highest potential for renewable heat in the district bears the development of environmental heat of the adjacent river. The river temperature drops to values between 0 and 10 °C in winter, while in summer it can rise to just over 20 °C. The river heat is therefore available at a just sufficient temperature level to be used by a heat pump and fed into the subnetwork of the district. The necessary river water extraction points already exist at the CHP plant site including the corresponding permit to use the river water for CHP cooling. In this context, the river temperature may be increased by up to 3 K to a maximum of 28 °C. After consultation with the utility, no major obstacles are to be expected for an extension of this permit for heating purposes. Cooling the currently maximum permissible volume flow by only 2 K corresponds to a thermal capacity of 50 MW.

A schematic diagram of the integration concept at the CHP plant site is depicted in Fig. 2. Part of the volume flow of the river water is redirected through a shell-and-tube heat exchanger. The river water heat is then transferred to an intermediate cycle (70 % water, 30 % glycol) to prevent contact between the refrigerant of the heat pump and the river water. In the case at hand suitable refrigerants are ammonia (R717) and hydrofluorolefins (HFOs), which are both characterized through very low global warming potentials. Within the case study ammonia was chosen as refrigerant due to its higher efficiency compared to HFOs according to Jesper et al. (2021). As the temperature lift ranges from 53 K in the summer up to 86 K in the winter, it is also more efficient to use a two-stage heat pump. The seasonal performance factor (SPF) estimated for this use case with a method developed by Jesper et al. (2021) is 2.3 for a single-stage versus 3.0 for a two-stage system. The heat pump is connected to a tank thermal energy storage (TTES), that can be charged with up to 90 °C. When the heat load of the subnetwork exceeds the maximum heat output of the TTES, the residual load is covered by the primary DH network through a district substation. In this case a smart control strategy is to be developed that maximizes the efficiency of the heat pump by setting the optimized

volume flows and supply temperatures of the heat pump and the post-heating with the district substation.

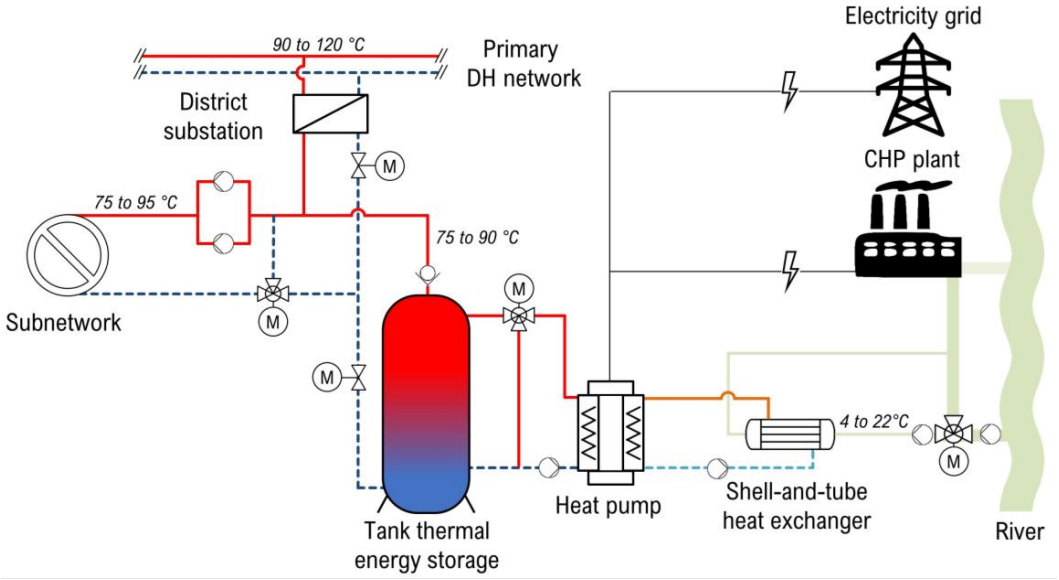

Fig. 2: Integration of a river water heat pump (schematic diagram)

2.3 Potential for solar thermal heat

The lack of open spaces in the district only leaves the option of decentralized rooftop systems in terms of solar thermal heat. According to Heymann et al. (2019) the minimum collector area of solar thermal systems feeding into the DH network should be 200 m² due to the complexity as well as high investment and operating costs. To determine the total potential collector area in the district, large rooftops were analyzed systematically with the help of the city's solar map and 3D-scans of the buildings. After applying the exclusion criteria of a minimum collector area of 200 m² per system and a minimum collector area of 350 m² per building complex, a total potential of 8,300 m² could be identified. Nevertheless, the feasibility of the systems is strongly dependent on individual local conditions, so that those buildings with the highest implementation probability were selected by the utility according to Tab. 1. The final selection amounts to a total collector area of 4,841 m².

Tab. 1: Potential collector areas of solar thermal rooftop systems

ID	Inclination	Orientation*	Collector Area
01	0°	+30°	504 m²
02	0°	-15°	525 m²
03	0°	-2°, 0°	463 m²
04	30°	-90°	848 m²
05	0°	+10°	384 m²
06	0°	-15°	1590 m²
07	0°	-15°	526 m²
* -90° = East; 0° = South; +90° = West			

2.4 Heat supply concepts

Within the case study the following three concepts are compared regarding operational characteristics and economic efficiency (see Fig. 3). The core element to achieve the required cover ratio of 50 % renewable energies in all three concepts is the river water heat pump in combination with a TTES. In all cases the primary network covers the residual load and serves as a backup but is hydraulically separated from the subnetwork through a district substation. In Concept II, the heat pump is complemented by the decentralized solar thermal rooftop systems, that feed directly into the supply line of the grid using individual feed-in stations. Concept III consists of additional CHP and Power-to-Heat (PtH) units to account for the sector coupling aspects of heat production.

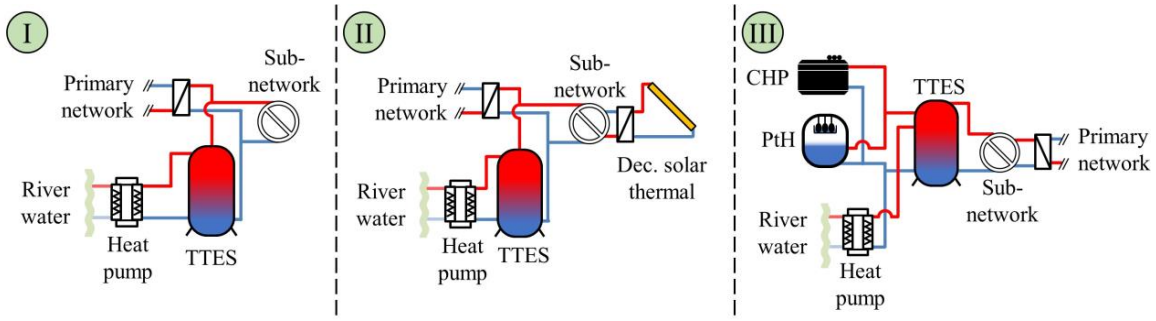

Fig. 3 Schematic diagrams of three heat supply concepts

The heat production components are designed to still reach a 50 % renewable cover ratio in the year 2030, when the peak in heat demand is expected. The resulting dimensions are shown in Tab. 2.

Tab. 2: Component dimensions

Component	Concept I	Concept II	Concept III
Heat pump	4.7 MW_{th}	4.7 MW_{th}	6.2 MW_{th}
Solar thermal systems	-	4,841 m²	-
CHP unit	-	-	7.12 MW_{th}; 7.2 MW_{el}
PtH unit	-	-	2.2 MW_{th}
Storage	600 m³	600 m³	7000 m³

It must be noted that although there are additional decentralized solar thermal systems in Concept II, the heat pump needs the same heat output as in Concept I. This is resulting from the sole availability of solar heat during low heat load periods in summer, while the contribution of the heat pump in winter is decisive to reach the desired renewable cover ratio. In Concept III, a goal of the design is to achieve a very flexible heat production with a focus on electricity market prices. The CHP unit is designed to only operate 3,000 full load hours per year, but it still partially displaces renewable heat when electricity prices are high. In turn, the heat pump requires a larger heat output for periods with low electricity prices to reach the same desired renewable cover ratio as in Concept I and II. While the smaller storages in Concept I and II are short-term storages to shift daily summer loads, the much larger storage volume in Concept III is driven by a minimum requirement in the subsidy program in combination with CHP units.

2.5 Framework for the economic comparison of the heat supply concepts

The relevant expenses for the economic comparison include investments, fuel costs as well as maintenance and service costs for the respective components mentioned in section 2.4. On these grounds the Levelized Cost of Heat (LCoH) for each concept is calculated. According to Baez and Larriba Martinez (2015) LCoH is “the constant and theoretical cost of generating one kWh of heat, which is equal to the discounted expenses incurred throughout the lifetime of the investment” and is determined following equation 1. The required input variables are discussed in the following.

$$LCoH = \frac{I + \sum_{t=1}^{T} \frac{C_t - S_t - RV}{(1+i)^t}}{\sum_{t=1}^{T} \frac{E_t}{(1+i)^t}} \qquad \text{(eq. 1)}$$

$LCoH$	Levelized Cost of Heat [€/MWh]	S_t	Revenue from operation [€]
I	Investment costs [€]	RV	Residual value [€]
T	Assessment period [-]	i	Discount rate [%]
t	Year [-]	E_t	Produced heat [MWh]
C_t	Operating costs [€]		

The assessment period (T) is 15 years and equals the simulation period (see section 3.1). The investment costs (I) for the components are shown as specific values in Tab. 3. The program “Wärmenetzsysteme 4.0” grants a 30 % subsidy on the investments. Hence, the total investment is lowest in Concept I with 2.25 M€, about 4.93 M€ in Concept II due to the additional solar thermal systems and 8.74 M€ in Concept III, where the most and largest components are planned.

Tab. 3: Specific turn-key investment costs

Component	Specific investment costs			Reference
	Concept I	Concept II	Concept III	
Heat pump	578 €/kW$_{th}$	578 €/kW$_{th}$	558 €/kW$_{th}$	Manufacturer information; Große et al. (2017); Wolf (2017)
Solar thermal systems	-	790 €/m²	-	Heymann et al. (2019)
PtH unit	-	-	180 €/kW$_{th}$	Große et al. (2017)
CHP unit	-	-	654 €/kW$_{el}$	Klein et al. (2014)
Storage	830 €/m³	830 €/m³	561 €/m³	Große et al. (2017)

The operating costs (C_t) include the fuel costs, but also costs for maintenance and service. The fuel costs are determined with the results of dynamic simulations (see section 3) and prognoses for specific costs of electricity and natural gas. The prognoses were provided by the utility and are based on energy market models by the company Prognos AG. Thus, the mean electricity spot market price ranges from 58.3 €/MWh in the year 2024 up to 72.8 €/MWh in 2038. It is assumed that the heat pump is driven by self-generated electricity from the CHP plant. Therefore, the lost revenue from a potential electricity feed-in is considered as electricity costs. Additionally, German legislation requires 40 % of the renewable energy levy to be paid for self-generated electricity consumption in this case. The levy is expected to be at 58.9 €/MWh in the year 2024 and decreases to 13.6 €/MWh until 2038. The forecasted natural gas price is at 39.1 €/MWh in 2024 and increases to 47.2 €/MWh until 2038. This already includes a tax on CO_2-emissions, which is assumed to be at 45 €/t_{CO2} in 2024 and increases to 68 €/t_{CO2} in 2038. The costs for maintenance and service of the components are assumed according to the references listed in Tab. 3. The revenue from operation (S_t) is only relevant in Concept III, where the fed-in electricity of the CHP unit is remunerated according to electricity spot market prices. It is assumed that the storages and the solar thermal systems have a useful life of 25 years, which exceeds the assessment period. Therefore, their residual value (RV) is taken into consideration for calculating the LCoH. This is not relevant for the heat pump, the CHP and the PtH unit, as a useful life of 15 years is assumed for those components. The discount rate (i) was chosen at 8 %. Finally, the heat (E_t) that is produced by the new components is considered.

3. Simulation of heat production

As a focus of the concept comparison is on electricity market price induced heat production, the software energyPRO is used to simulate long-term operation of the components on an hourly basis. The software enables a simple integration of time series, including a prognosis of electricity spot market prices, weather data (ambient temperature, river temperature, soil temperature) and its respective expected developments in the future. The heat production components are prioritized for every timestep with the time series as boundary conditions. The software uses an analytical optimization method to find the best solution for meeting the heat demand while utilizing the available storage capacity. In contrast, the complexity of decentralized solar thermal systems feeding into a DH system cannot be modelled in energyPRO. Therefore, the software Polysun is used to simulate the solar thermal feed-in and is afterwards transmitted to energyPRO as a time series.

3.1 Boundary conditions of the energyPRO model

The most important boundary conditions for the simulation of heat production are laid out in the following. The simulation period is 15 years starting from the year 2024 until 2038. A corresponding prognosis for ambient temperatures was generated with the software Meteonorm. Based on the correlation between historical ambient temperature and river temperature at the CHP plant site, a prognosis for the river temperature was modelled. Furthermore, the supply and return temperature of the subnetwork of the DH system were implemented as a function of ambient temperature (see Fig. 4). The depicted supply temperature curve reflects a mean temperature decrease of 19 K compared to the supply temperature of the primary network.

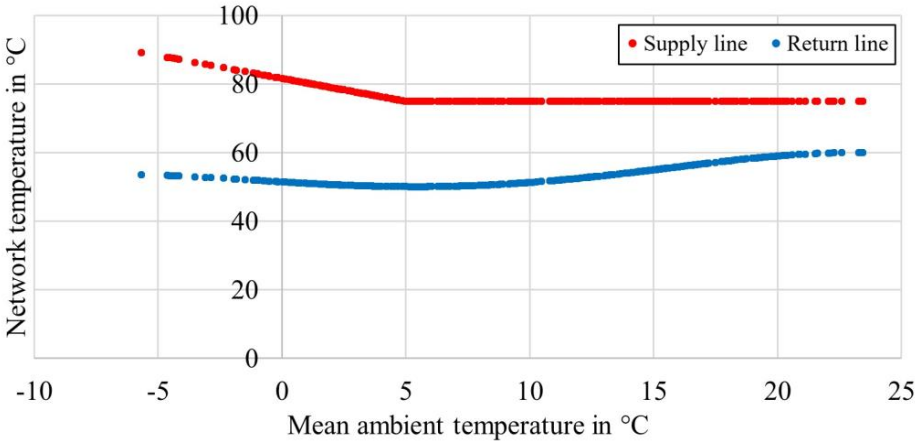

Fig. 4: Network operating temperatures

The temperature difference between supply line of the subnetwork and the river is crucial to predict the efficiency of the heat pump. For this purpose, a method by Jesper et al. (2021) was applied, that enables to estimate the coefficient of performance (COP) as a function of temperature lift between heat source and heat sink of the heat pump. The hourly prediction of the COP was then considered as a boundary condition in the simulation model and for the calculation of electricity costs. It is assumed that the electricity for the heat pump as well as the electricity export of the CHP unit is directly traded at a spot market. The relevant long-term time series of hourly electricity spot market prices is retrieved from the prognosis mentioned in section 2.5.

The simulation model considers the hourly heat load curves for all customers as well as network losses. The annual heat demand was allocated to the days of the year depending on mean ambient temperatures of the reference year 2020. The allocation relies on standard load profiles according to Hellwig (2003) and the respective further development by Hinterstocker et al. (2015). The used profiles correspond to residential and non-residential buildings. Measurements of the actual heat load in the district were used to create hourly profiles from the allocated daily heat demands. The resulting heat load profiles for the residential and non-residential buildings connected to the subnetwork can be seen in Fig. 5. Additionally, the load profile for the network losses was modelled using the heat transfer coefficient area product (UA-value) of the heating network and the difference between network and soil temperature. Due to the lowered supply temperatures in the subnetwork, it is assumed that the heat losses are reduced from 14.5 % to 12.3 % of the heat feed-in.

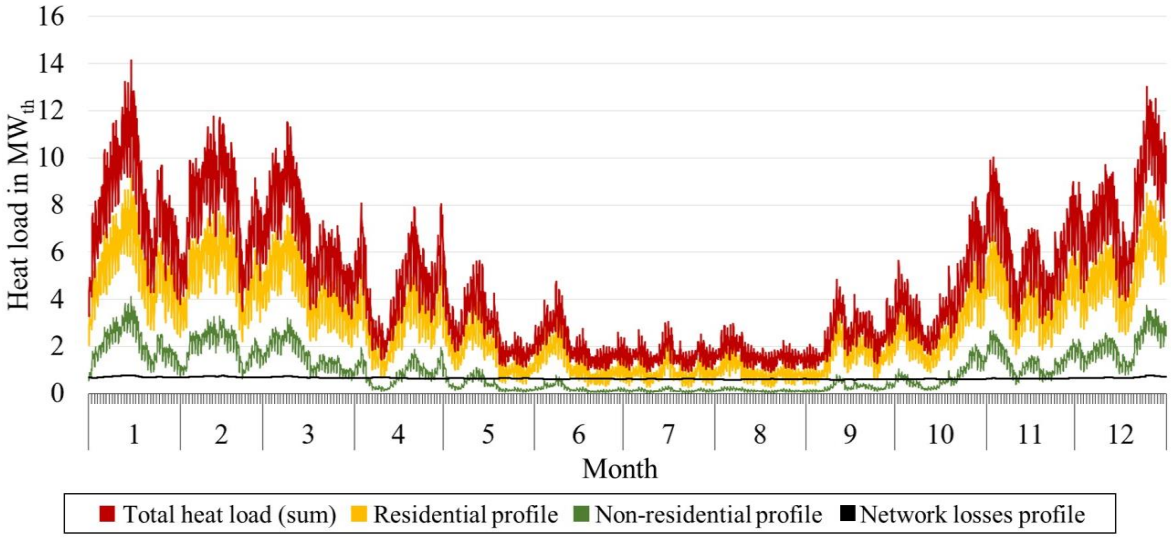

Fig. 5: Hourly total heat load and consumption profiles as course of the year

3.2 Simulation of solar thermal feed-in

The software Polysun offers a model template to simulate the direct feed-in of solar thermal systems into the supply line of DH networks. The model was adapted to the given use case using the configuration guidelines described by Schäfer et al. (2015). Seven representative models were configured with respect to the identified potential systems

in section 2.3. This includes collector area, pipe lengths, orientation, inclination, shading, and temperatures. CPC vacuum tube collectors were chosen as collector type. The operation of the representative models was then scaled to the total potential collector area. The resulting annual profile can be seen in Fig. 6. The total potential solar thermal feed-in amounts to 1,824 MWh/a. With a collector area of only 4,841 m² the expected excess heat, that would require a storage, is only 2,4 % of the total feed-in. Furthermore, it can be observed that due to row shading and higher supply temperatures (> 80°C) in winter, there is almost no feed-in from November until February. The specific yields of the seven representative systems range from 336 to 391 kWh/m²·a. A subsequent thermohydraulic simulation of the heating network, that was conducted by the utility, verified the feasibility of the solar thermal feed-in.

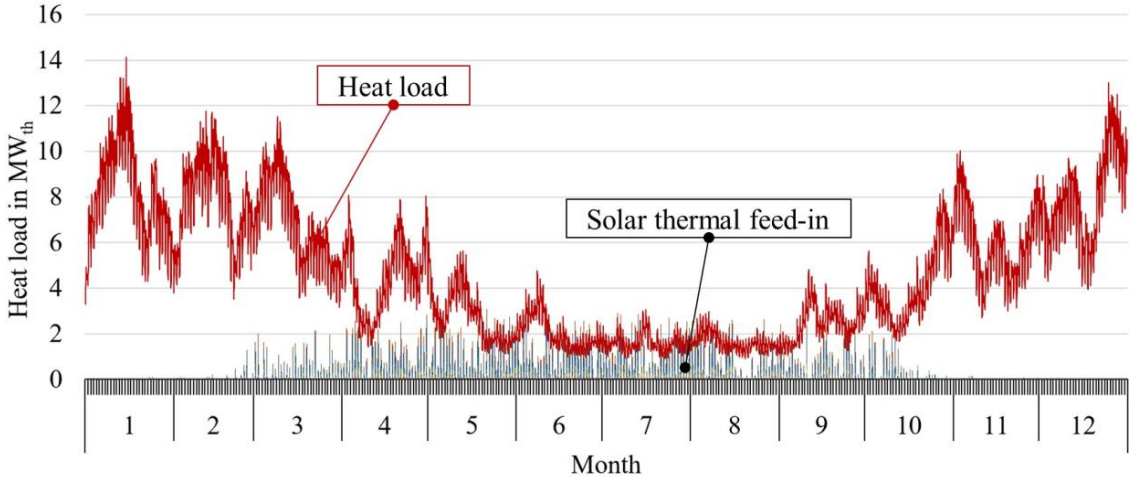

Fig. 6: Hourly solar thermal feed-in and total heat load as course of the year

3.3 Simulation results

The resulting key figures of the energyPRO simulation are shown as mean values of the 15-year simulation period in Tab. 4. The desired renewable cover ratio of a minimum of 50 % is reached in all three concepts throughout the entire simulation period. The additional solar thermal heat in Concept II leads to a slightly lower cover ratio of the heat pump compared to Concept I. With an additional CHP unit in Concept III, the primary network only covers the peak loads with a cover ratio of 5.7 %. The PtH unit just covers 0.5 % due to a limitation in the operation strategy to run at negative electricity market prices. As a result of the larger heat pump and storage in Concept III, a more flexible operation of the heat pump can be seen. The full load hours (FLH) are significantly lower than in Concept I and II. The seasonal performance factor (SPF) is almost identical in all cases. In the course of a year, the coefficient of performance (COP) can get as low as 2.50 in winter, while it reaches up to 3.45 during the summer. Even though the storage in Concept III is almost 12-times larger than in Concept I and II, the storage cycles still indicate an acceptable utilization.

Tab. 4: Concept comparison - Simulation results

Key figure		**Concept I**	**Concept II**	**Concept III**
Cover ratio	*Heat pump*	53.4 %	50.9 %	54.7 %
	Solar thermal	-	3.3 %	-
	PtH unit	-	-	0.5 %
	CHP unit	-	-	39.1 %
	Primary network	46.6 %	45.8 %	5.7 %
FLH heat pump		6,120 h/a	5,828 h/a	4758 h/a
SPF heat pump		3.05	3.04	3.04
FLH CHP unit		-	-	2961
Storage cycles		225 cycles/a	233 cycles/a	59 cycles/a

4. Opportunities for sector coupling

In the following the three heat supply concepts are analyzed regarding their electricity market price induced operation. For this purpose, mean daily operations within the 15-year simulation period are shown in Fig. 7 to Fig. 11. The possibility to adapt the heat production according to electricity market prices is strongly dependent on the month of the year. In the summer, when the heat load is driven by domestic hot water demand and reaches only 15 to 20 % of the winter load, the heat pump is much more flexible to run at low market prices and utilize the storage.

In July (see Fig. 7 to Fig. 9), the mean electricity market price shows a significant dip around noon. This can be traced back to the feed-in of a large amount of solar PV-systems in Germany, that usually peaks around noon. The mean operation of the heat pump in Concept I (see Fig. 7) adapts to this dip and loads the storage (blue/yellow shaded bars) around noon. The same is true for the operation during the night, although the market price does not drop as much here. This indicates that the heat output of the heat pump and storage size limit the flexible operation.

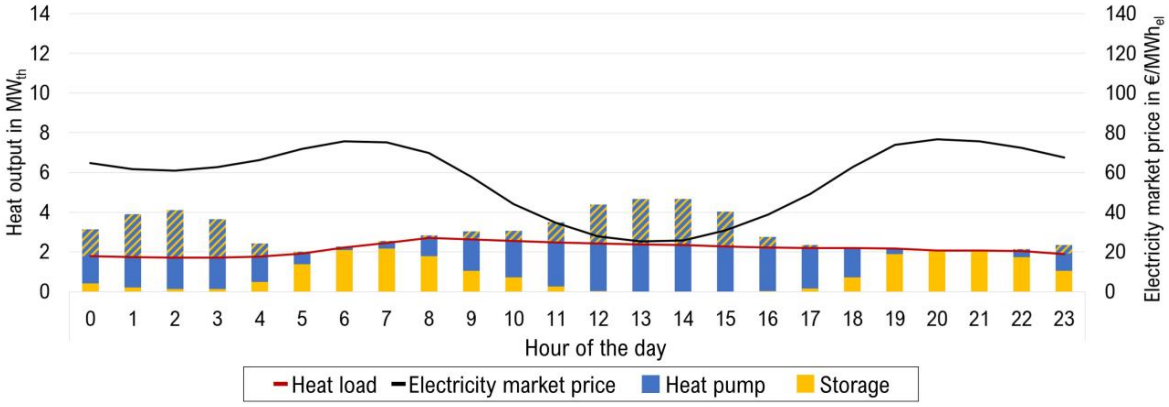

Fig. 7: Concept I - Mean daily operation in July

In Concept II, the additional solar thermal heat primarily reduces the heat pump operation at low market prices and high COPs in the summer (see Fig. 8), as their feed-in profile is almost identical to that of solar PV-systems into the electricity grid. The solar thermal peak is slightly before noon because most of the identified potential collector areas in section 2.3 are oriented to the east or southeast.

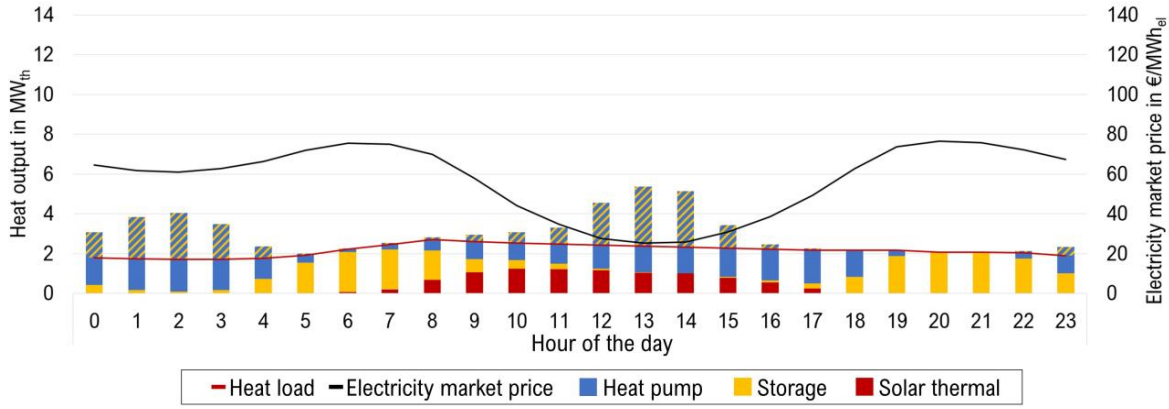

Fig. 8: Concept II - Mean daily operation in July

In contrast to Concept I and II, the combination of a larger heat pump and storage in Concept III enables a more extensive utilization of the market price dip around noon. Even the operation at night is at a minimum here (see Fig. 9).

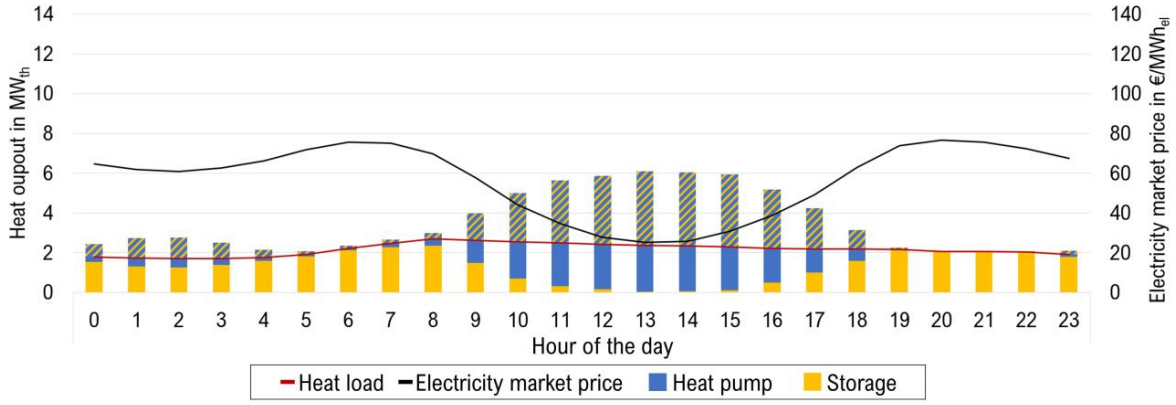

Fig. 9: Concept III - Mean daily operation in July

In Fig. 10 the mean daily operation of Concept III in October is shown as an example for the transitional periods. The mean daily course of the electricity market price is now characterized by a morning and evening peak, while the dip at noon caused by solar PV feed-in declines.

The heat load of the heating network in the spring and fall is about twice as high as in the summer due to additional space heating demand. Therefore, the flexibility of the systems decreases especially in Concepts I and II. Nevertheless, the mean daily profiles show, that an operation of the heat pump during the morning and evening market price peaks is still prevented to the extent possible. As depicted in Fig. 10, this operational characteristic can particularly be seen in Concept III. Additionally, the CHP unit supports this operation by following the opposite course of the heat pump producing heat and electricity when market prices are high.

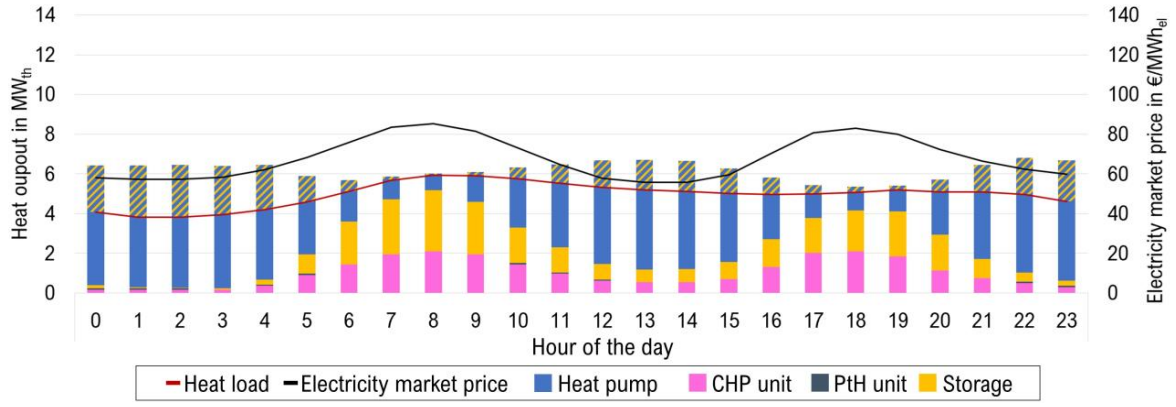

Fig. 10: Concept III - Mean daily operation in October

When the heat load is reaching its maximum in winter, the flexibility of the systems declines. As shown in Fig. 11, the mean electricity market price in January is characterized by low prices at night as well as the morning and evening peaks. In Concept III, the CHP unit still feeds in most during those peaks, but the operation of the heat pump does not seem to be affected by the market price anymore. In that context it must be noted that the mean heat output of the heat pump in January is significantly lower at only 2 to 3 MW_{th} compared to the maximum of 6.2 MW_{th} during the summer. This effect is caused by periods with very low river temperatures below 4 °C. During those periods, the heat pump cannot operate at all due to technical limitations, so that the mean heat output decreases.

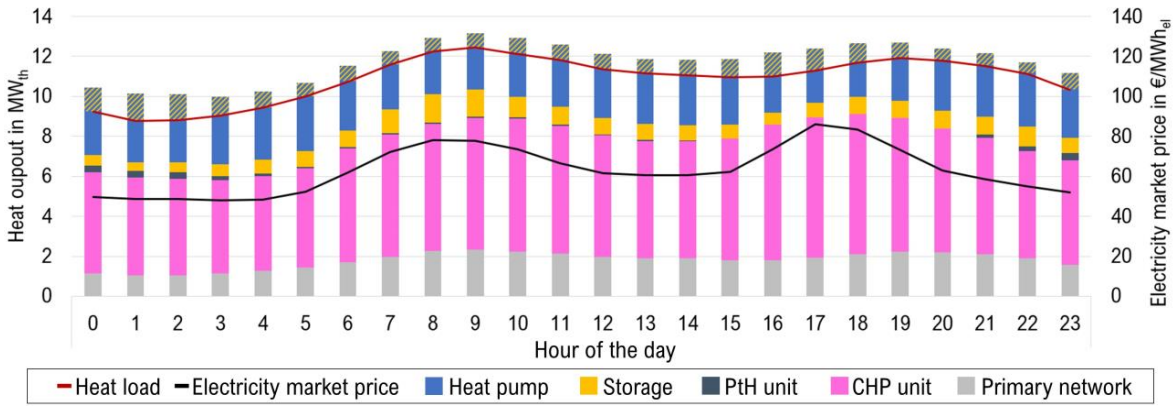

Fig. 11: Concept III - Mean daily operation in January

As a key figure to summarize and reflect on the conducted analysis, the mean deviation (d) of the consumption and feed-in of electricity from mean market price ($\bar{c}_{el,market}$) is considered. It is calculated according to equation 2 and 3 with the cost of electricity ($C_{el,HP}$) and the electricity consumption ($E_{el,HP}$) of the heat pump, respectively the revenue ($S_{el,CHP}$) and the exported electricity ($E_{el,CHP}$) of the CHP unit.

$$d_{consumption} = \left(\frac{\frac{C_{el,HP}}{E_{el,HP}}}{\bar{c}_{el,market}} - 1 \right) * 100\% \qquad \text{(eq. 2)}$$

$$d_{feed-in} = \left(\frac{\frac{S_{el,CHP}}{E_{el,CHP}}}{\bar{c}_{el,market}} - 1 \right) * 100\% \qquad \text{(eq. 3)}$$

$d_{consumption}$	Mean deviation of the consumption of electricity from mean market price [%]
$d_{feed-in}$	Mean deviation of the feed-in of electricity from mean market price [%]
$C_{el,HP}$	Cost of electricity for the heat pump [€]
$E_{el,HP}$	Electricity consumption of the heat pump [MWh_{el}]
$S_{el,CHP}$	Revenue from feed-in of electricity of the CHP unit [€]
$E_{el,CHP}$	Exported electricity of the CHP unit [MWh_{el}]
$\bar{c}_{el,market}$	Mean electricity market price [-]

The deviation concerning the electricity consumption of the heat pump is quite low in Concept I with -3.5 % and Concept II with -2.7 %. The slightly lower deviation in Concept II is consistent with the observations made in Fig. 8. The more flexible operation in Concept III leads to a significant deviation of -15.5 %. This shows that a flexible operation in transitional periods is necessary to achieve significantly lower market prices for electricity consumption. The same applies to the feed-in of electricity by the CHP unit in Concept III, which is even at +23.6 %.

5. Economic comparison of heat supply concepts

The LCoH for the three concepts are depicted in Fig. 12. The corresponding economic framework conditions are laid out in section 2.5. The lowest LCoH are achieved in Concept I with 36.7 €/MWh. Here, electricity costs account for the largest share with 68 %, while the investment for the heat pump and the storage is only 25 % of the total. The LCoH in Concept II is 45.8 €/MWh and therefore almost 25 % higher than in Concept I. The largest cost component is still the electricity for the heat pump with 52 % of the LCoH. Despite that the share of the investment costs for the decentralized solar thermal system is 19 % of the LCoH and therefore causes the significant deviation from Concept I. Considering that the solar thermal systems only achieve a cover ratio of 3.3 %, an economic efficiency is not given. The flexible electricity market price induced operation in Concept III leads to lower shares of the electricity costs, but also for natural gas for the CHP unit as revenue from electricity feed-in is generated. Nevertheless, this is not reflected in the LCoH of 44.6 €/MWh, which are 21.5 % higher than in Concept I due to the high total investment volume for additional components. In this context the requirement for the large storage volume in the subsidy program in connection with CHP units must be noted.

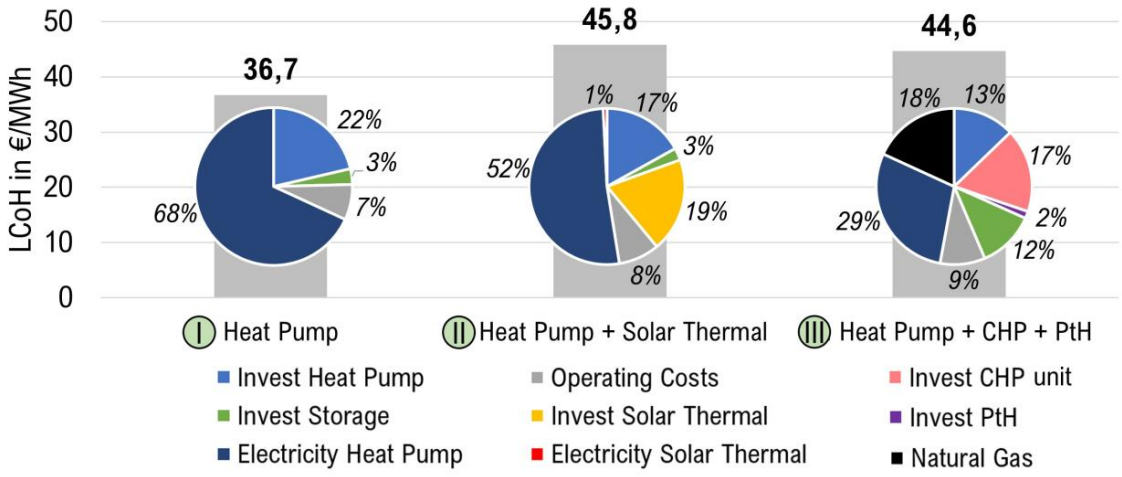

Fig. 12: Concept comparison - Levelized Cost of Heat (LCoH)

6. Discussion

In this paper, the integration of a river water heat pump at an existing CHP plant site was illustrated and analyzed in terms of technical and economic aspects. In a densely populated area this presents an excellent opportunity for the decarbonization of urban DH systems. In addition, the shown concept can be scaled by extending the heat pump feed-in to the primary DH network, as only 5 % of the theoretically available heat flow from the river was considered in the case study. Three different heat supply concepts were designed combining the river water heat pump with decentralized solar thermal rooftop systems as well as a CHP and PtH unit. 15-year dynamic simulations were used to investigate how the shown use case can support the energy system transformation process by aligning heat production with electricity spot market prices. As the prognosis for market prices is heavily dependent on external conditions, further investigations with different scenarios for the development of the electricity sector should be conducted. In that context the framework for heat pumps operated with net electricity plays an important role. The economic efficiency of very flexible heat production systems could be further improved if the cost of electricity bears even more flexible price components like grid usage charges and system services.

The conducted case study shows that the system with the least components to meet the 50 % renewable cover ratio is the most cost efficient with the underlying subsidy program “Wärmenetzsysteme 4.0” (BAFA, 2020). The integration of decentralized solar thermal systems is cost intensive, which leads to the conclusion that the potential for large on-ground collector fields should be exploited first. It is important to keep in mind that the goal of 50 % renewable cover ratio is only an intermediate milestone to an all renewable scenario. In this light, the shown Concept III gives an outlook on how green fuels could be used in smaller decentralized CHP units in the future.

7. References

AGFW e.V., 2019. AGFW-Hauptbericht 2018. AGFW e.V., Frankfurt am Main, Germany.

Baez, M. J., Larriba Martinez, T., 2015: Technical Report on the Elaboration of a Cost Estimation Methodology. Work Package 3 – Estimating RHC energy costs. Creara. Madrid, Spain.

BAFA, 2020. Modellvorhaben Wärmenetzsysteme 4.0. https://www.bafa.de/DE/Energie/Energieeffizienz/Waermenetze/waermenetze_node.html;jsessionid=59C35C9BB1737E484CC479F94B8C1571.1_cid381. Accessed 31 August 2020. Bundesamt für Wirtschaft und Ausfuhrkontrolle, Eschborn, Germany.

Frederiksen, S., Werner, S., 2017. District heating and Cooling, first ed. Studentlitteratur, Lund, Sweden.

Große R, Christopher B, Stefan W, Geyer R, Robbi S, 2017. Long term (2050) projections of techno-economic performance of large-scale heating and cooling in the EU: external study performed by ILF Consulting Engineers Austria GmbH and AIT Austrian Institute of Technology GmbH for the Joint Research Centre. Publications Office of the European Union, Luxembourg.

Hellwig, M., 2003. Entwicklung und Anwendung parametrisierter Standard-Lastprofile. Institute of Power Engineering. Dissertation. TU Munich, Munich, Germany.

Heymann, M., Rosemann, T., Rühling, K., Hoppe, S., Wudenka, E., Hafner, B., 2019. Kostenreduktionspotential beim Ausbau der Solarisierung von Fernwärmenetzen durch Standardisierung. TU Dresden and Viessmann Werke GmbH & Co. KG. Dresden, Allendorf, Germany.

Hinterstocker, M., Eberl, B., v. Roon, S., 2015. Weiterentwicklung des Standardlastprofilverfahrens Gas. Forschungsgesellschaft für Energiewirtschaft mbH (FfE), München, Germany.

Jesper, M., Schlosser, F., Pag, F., Walmsley, T.G., Schmitt, B., Vajen, K., 2021. Large-scale heat pumps: Uptake and performance modelling of market-available devices. Renewable and Sustainable Energy Reviews. 137, 110646.

Klein, C., Rozanski, K., Gailfuß, M., Kukuk, J. Beck, T., 2014. BHKW-Kenndaten 2014/2015. Module, Anbieter, Kosten. ASUE Arbeitsgemeinschaft für sparsamen und umweltfreundlichen Energieverbrauch e.V., Berlin, Germany.

Schäfer, K., Mangold, D., Pauschinger, T., 2015. DEZENTRAL – Dezentrale Einspeisung in Nah- und Fernwärmesysteme unter besonderer Berücksichtigung der Solarthermie. Teilbericht des Verbundpartners Solites. Forschungsbericht zum Forschungsvorhaben 03ET1039C. Steinbeis Forschungsinstitut für solare und zukunftsfähige thermische Energiesysteme, Stuttgart, Germany.

Schweikardt, S., Didycz, M., Engelsing, F., Wacker, K., 2012. Sektoruntersuchung Fernwärme. Bundeskartellamt, Bonn, Germany.

Wolf, S., 2017. Integration von Wärmepumpen in industrielle Produktionssysteme. Institute of Energy Economics and Rational Energy Use. Dissertation. University of Stuttgart, Stuttgart, Germany.